

# VTAM: Video-Tactile-Action Models for Complex Physical Interaction Beyond VLAs

Haoran Yuan<sup>1,\*</sup>, Weigang Yi<sup>1,\*</sup>, Zhenyu Zhang<sup>2,\*</sup>, Wendi Chen<sup>3,\*</sup>

Yuchen Mo<sup>1</sup>, Jiashi Yin<sup>1</sup>, Xinzhuo Li<sup>1</sup>, Xiangyu Zeng<sup>1</sup>

Chuan Wen<sup>3</sup>, Cewu Lu<sup>3</sup>, Katherine Driggs-Campbell<sup>1</sup>, Ismini Lourentzou<sup>1,†</sup>

<sup>1</sup>University of Illinois Urbana-Champaign <sup>2</sup>Stanford University <sup>3</sup>Shanghai Jiao Tong University

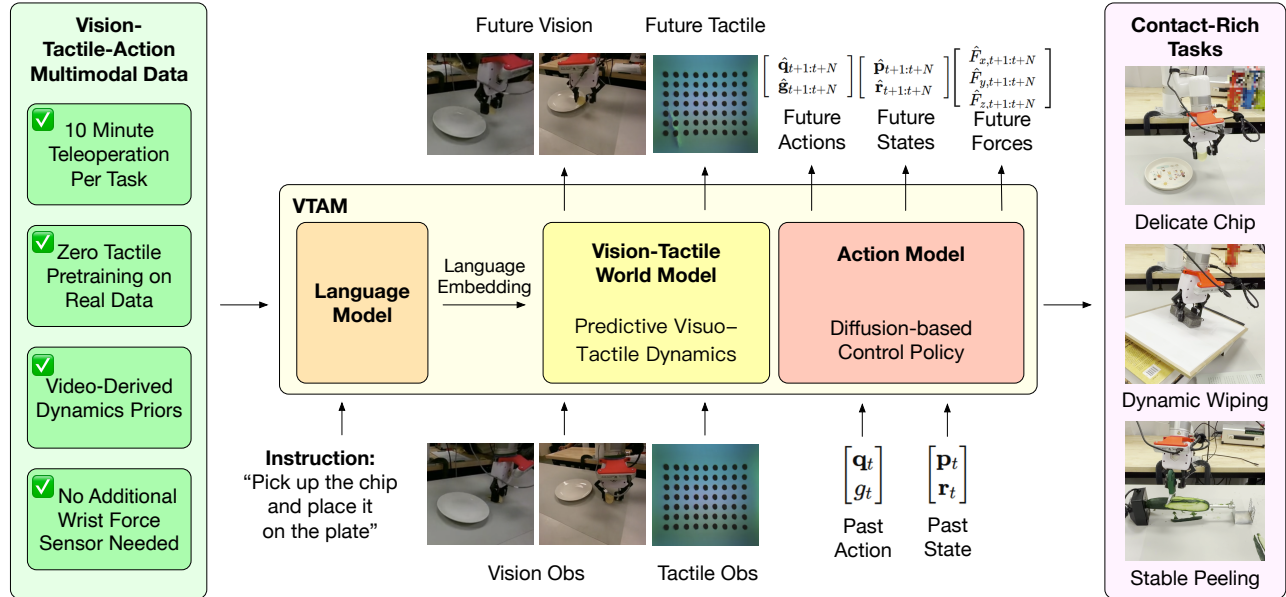


**Figure 1:** We introduce VTAM, a generalist Video-Tactile Action Model that integrates tactile sensing into a predictive video world model. By grounding control in visuo-tactile dynamics and force-aware reasoning, VTAM enables stable control in diverse contact-rich scenarios.

**Abstract.** Video-Action Models (VAMs) have emerged as a promising framework for embodied intelligence, learning implicit world dynamics from raw video streams to produce temporally consistent action predictions. Although such models demonstrate strong performance on long-horizon tasks through visual reasoning, they remain limited in contact-rich scenarios where critical interaction states are only partially observable from vision alone. In particular, fine-grained force modulation and contact transitions are not reliably encoded in visual tokens, leading to unstable or imprecise behaviors. To bridge this gap, we introduce the Video-Tactile Action Model (VTAM), a multimodal world modeling framework that incorporates tactile perception as a complementary grounding signal. VTAM augments a pretrained video transformer with tactile streams via a lightweight modality transfer finetuning, enabling efficient cross-modal representation learning without tactile-language paired data or independent tactile pretraining. To stabilize multimodal fusion, we introduce a tactile regularization loss that enforces balanced cross-modal attention, preventing visual latent dominance in the action model. VTAM demonstrates superior performance in contact-rich manipulation, maintaining a robust success rate of 90% on average. In challenging scenarios such as potato chip pick-and-place requiring high-fidelity force awareness, VTAM outperforms the  $\pi_{0.5}$  baseline by 80%. Our findings demonstrate that integrating tactile feedback is essential for correcting visual estimation errors in world action models, providing a scalable approach to physically grounded embodied foundation models.

<https://plan-lab.github.io/vtam>

## 1. Introduction

Recent advances in Vision–Language–Action (VLA) models have enabled generalist robot control through large-scale multimodal alignment [3, 17, 49]. By embedding visual observations and language instructions into a shared semantic latent space, these models can generalize across diverse manipulation tasks and environments [9, 30]. However, while vision supports high-level semantic understanding and language specifies task intent, *physical interaction is fundamentally governed by tactile feedback*, the only modality that directly encodes instantaneous contact dynamics between the robot and its environment. Tactile sensing is particularly critical for fine-grained, contact-rich manipulation, such as handling fragile, deformable, or slippery objects. Unlike vision, which captures relatively stable object geometry from a distance, tactile signals reflect the transient spatiotemporal evolution of forces at the contact interface. Effective use of this modality requires not only spatial reasoning over force distributions but also temporal reasoning over how these distributions evolve under dynamic interaction.

Most existing tactile-augmented VLA architectures incorporate tactile information by either (1) projecting tactile embeddings into a pre-trained vision–language latent space, treating them as additional semantic tokens [37], or (2) concatenating tactile features with language-conditioned visual representations in the downstream policy [2, 11, 16]. While these approaches expose the model to tactile inputs, they place a substantial burden on representation learning: the model must implicitly infer contact physics within a semantic embedding space optimized for visual alignment and static scene description rather than physical prediction. Learning that particular tactile patterns correspond to slip, deformation, or instability requires discovering these concepts indirectly through static correlations. This often demands large-scale annotated data and offers no guarantee that the underlying high-frequency dynamics will be faithfully captured. Without explicit temporal modeling, these learned representations struggle to encode the causal relationships between successive tactile frames, precisely the structure needed to anticipate failure modes such as incipient slip [22, 32, 42]. Moreover, because many VLA backbones prioritize semantic alignment over predictive physical modeling, they further underutilize tactile signals for fine-grained spatial and temporal reasoning [2, 16].

We address these limitations by introducing **VTAM**, a generalist **V**ideo–**T**actile **A**ction **M**odel that integrates tactile sensing into a predictive world-model framework for contact-rich manipulation, as shown in Fig. 1. At the representation level, we design a visuo–tactile predictive module built on top of a pretrained video backbone. Instead of mapping tactile signals into a language-aligned semantic space, VTAM treats touch as a primary sensory modality and jointly predicts the future evolution of visual and tactile streams conditioned on the robot’s end-effector state. This predictive formulation enables the backbone to learn temporally consistent visuo–tactile features without requiring explicit semantic annotations of contact events. Furthermore, at the action-learning level, we address the modality collapse problem that commonly arises when integrating tactile inputs into action training. By introducing a virtual force prediction objective at the action head, we regularize multimodal fusion and stabilize training. This design encourages the policy to maintain sensitivity to tactile signals during action optimization, effectively preventing the dominance of visual features.

We validate VTAM on three diverse contact-rich manipulation tasks: chip pick-and-place, peeling, and wiping. On the chip pick-and-place task, VTAM achieves a 90% success rate, compared to 0% for the vision-only baseline and 10% when removing the virtual force regularization. A naive downstream force integration without predictive visuo–tactile modeling fails entirely (0% success). Similar trends are observed across the peeling and wiping tasks, demonstrating that predictive visuo–tactile representation learning combined with action-level regularization substantially improves stability and task success. In summary, our main contributions are:

- We introduce **VTAM**, a visuo–tactile world action model that integrates high-resolution tactile sensing with visual observations within a predictive video backbone to enable robust contact-rich robotic manipulation.

- We propose a **joint visuo–tactile prediction framework** that forecasts future visual and tactile streams in a shared latent space, enabling the model to learn temporally consistent contact dynamics without requiring explicit semantic annotations.
- We introduce a **virtual force prediction objective** that successfully mitigates modality collapse during training, yielding empirical improvements over vision-only and naive integration baselines.
- We validate VTAM on challenging contact-rich robotic tasks, including potato chip pick-and-place, cucumber peeling, and whiteboard wiping with varying heights and tilt angles, demonstrating large improvements in success rate over vision-only and naive tactile baselines.

## 2. Related Works

**Vision-Language-Action Models.** VLA models have emerged as the dominant paradigm for generalist robot control, leveraging internet-scale vision–language pretraining to ground natural-language instructions in visual observations and decode motor commands through a unified architecture [3, 4, 17, 30, 49]. Subsequent efforts have expanded the paradigm along several axes, incorporating 3D geometric priors [28, 46], hierarchical task planning [1, 23], and predictive world knowledge [44, 47], consistently improving generalization and sample efficiency. Existing visuo-linguistic VLAs struggle with physical interactions when visual cues are occluded, particularly with fragile objects. VTAM targets this gap by incorporating high-resolution tactile observations directly into a generative world-model backbone: the model learns joint visuo–tactile dynamics and uses these representations to guide action generation, so tactile cues can correct visual misestimation during interaction and improve robustness on fragile and force-sensitive tasks.

**Generative World Models for Robotics.** Generative world models forecast future environment states to support planning and policy learning [26, 38]. Recent work has scaled this idea by jointly diffusing video and action trajectories [19]. DreamZero [39] builds a World Action Model on a pretrained video diffusion backbone, achieving zero-shot generalization and cross-embodiment transfer by learning physical dynamics from heterogeneous robot data. UWM [47] introduces modality-specific diffusion timesteps that decouple video and action noise schedules, enabling pretraining on large-scale datasets that include action-free video. DreamVLA [44] augments VLAs with future visual token prediction, and RDP [36] applies diffusion hierarchically for contact-aware action refinement.

Despite these advances, most existing world models encode environmental dynamics almost exclusively through visual prediction. While visual forecasting captures object motion and scene evolution, it provides only indirect access to the physical interaction signals that govern contact-rich manipulation. Critical phenomena such as slip, deformation, and force transfer arise at the contact interface and are often weakly observable or entirely hidden from camera views. As a result, models that rely solely on visual dynamics may struggle to anticipate failure modes during delicate or force-sensitive interactions. Motivated by this limitation, VTAM brings tactile deformation dynamics into the predictive world model and anchors control learning with a virtual-force target so the policy remains responsive when contact becomes visually ambiguous.

**Tactile Integration in Robotic Learning.** Tactile sensing provides direct access to contact physics and is essential for manipulation involving deformable, fragile, or occluded objects [14, 27]. On the representation side, contrastive objectives have been used to align visual and tactile embeddings [7, 13] or to learn sensor-agnostic tactile features [35]. At the policy level, recent methods incorporate tactile input through force-aware Mixture-of-Experts routing [40], dual-level feedback fusion [2], or tactile preference optimization [43]. These approaches, however, treat touch as a supplementary input channel fused reactively with vision rather than modeled predictively. A further practical challenge is modality collapse: visual gradients dominate

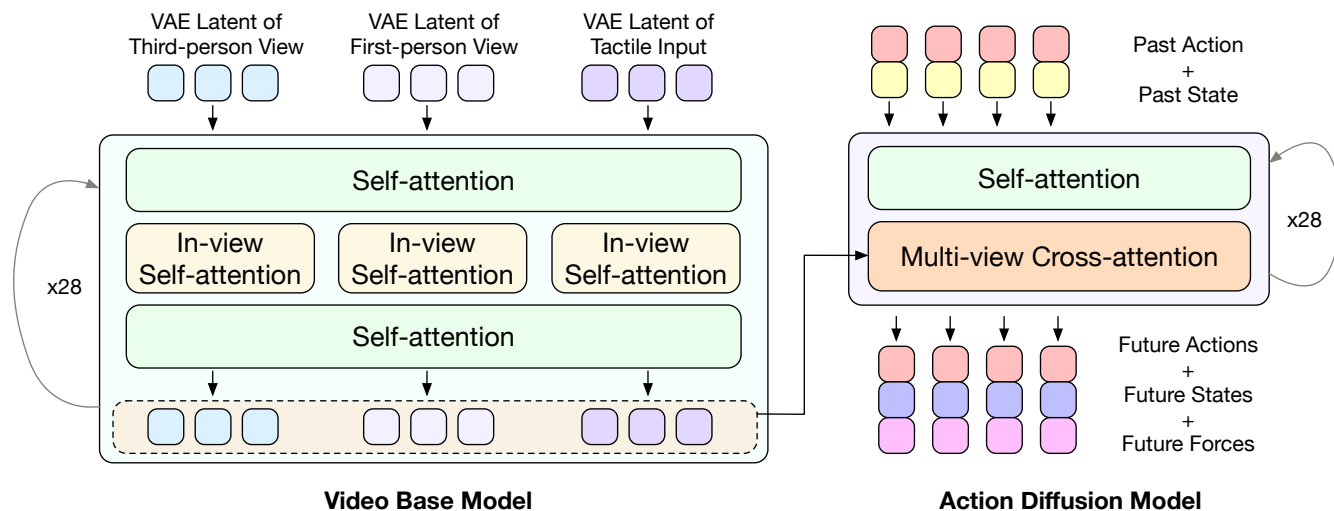


**Figure 2: VTAM Overview.** A pretrained video backbone jointly models multi-view visual and tactile latents via alternating intra-view and cross-view attention. The resulting multimodal representation is injected into a conditional action diffusion head to predict action, virtual force, and proprioceptive state.

during training and suppress the tactile or force signal [6, 20, 33, 34, 45]. Existing mitigations rely on explicit force-torque sensors [15] or hybrid position-force controllers [16], imposing hardware constraints that limit generality. VTAM departs from this reactive paradigm in two ways: it embeds tactile perception into the generative video backbone for joint visuo-tactile dynamics prediction rather than static fusion, and it introduces deformation-aware virtual force regularization at the action head to maintain tactile gradient influence throughout training without external force-torque hardware.

### 3. Method

We present the Video-Tactile Action Model (VTAM), a unified visuo-tactile world action model designed for contact-rich manipulation. As illustrated in Figure 2, VTAM operates by projecting both multi-view visual observations and high-resolution tactile streams (e.g., GelSight [41]) into a shared continuous latent space via a pre-trained Variational Autoencoder (VAE). Within this space, a multi-view diffusion process employing alternating intra-view and cross-view attention jointly models the temporal dynamics of the visual scene and the fine-grained physical deformations captured by the tactile sensor. The resulting multimodal representations encode predictive contact evolution. These representations are subsequently injected into a conditional diffusion-based action head via cross-attention, yielding temporally consistent and physically grounded control actions. Jointly optimizing visual and tactile modalities within a shared backbone often leads to modality collapse, in which dominant visual gradients suppress localized, high-frequency tactile signals. To address this fundamental optimization challenge, we introduce a deformation-aware virtual force regularization at the action head. This mechanism provides targeted supervision of the tactile pathway, thereby stabilizing multimodal fusion and ensuring that the policy remains sensitive to critical contact transitions during downstream tasks.

#### 3.1. Vision-Tactile Latent World Modeling via Multi-View Diffusion

A fundamental challenge in visuo-tactile modeling is preserving the high-frequency spatial details, such as subtle surface deformations and texture variations, that encode shear, slip, and pressure in tactile sensors

like GelSight [8, 41]. Standard semantic vision encoders [12] often discard these details in favor of coarse, object-level features. Therefore, we base our representation on a pretrained video Variational Autoencoder (VAE) [18, 31]. The reconstruction-oriented objective of the VAE provides a natural inductive bias that preserves fine-grained spatial and motion patterns [5]. This allows us to efficiently transfer modalities without designing a specialized tactile backbone. Beyond spatial details, effective contact manipulation requires understanding how forces evolve over time. Instead of routing tactile signals through lightweight, reactive downstream branches, we embed the tactile stream directly into a high-capacity video transformer. This architecture captures both the intra-frame deformation structure and the inter-frame contact evolution. Consequently, the model performs predictive reasoning over force trends, enabling it to anticipate critical transitions—a vital capability for handling brittle objects where failure occurs within millimeters of motion.

Formally, given an input frame  $\mathbf{I}_t^v$  at timestep  $t$  from view  $v$ , we use the pretrained video VAE encoder  $E$  to extract a continuous latent representation  $\mathbf{z}_t^v$ :

$$\mathbf{z}_t^v = E(\mathbf{I}_t^v), \quad v \in \{1, 2, 3\}, \quad (1)$$

where  $v=1, 2$  denote the third-person and first-person visual camera views, and  $v=3$  denotes the GelSight tactile stream. To model the complex spatial and inter-modal dynamics, we process these latents through a sequence of  $B$  alternating attention blocks. Let  $\mathbf{Z}_b = \{\mathbf{z}_{t,b}^1, \mathbf{z}_{t,b}^2, \mathbf{z}_{t,b}^3\}$  denote the set of latent tokens at the  $b$ -th block, with  $\mathbf{Z}_0$  being the initial VAE encodings. For each block  $b \in \{1, \dots, B\}$ , we first apply intra-view self-attention independently to each modality to capture spatial structures:

$$\tilde{\mathbf{z}}_{t,b}^v = \text{SelfAttention}(\mathbf{z}_{t,b-1}^v) \quad \forall v \in \{1, 2, 3\}. \quad (2)$$

Next, we concatenate the updated tokens across all views and apply a cross-view self-attention operation to model inter-modal interactions:

$$\mathbf{Z}_b = \text{CrossViewAttention}(\text{Concat}(\tilde{\mathbf{z}}_{t,b}^1, \tilde{\mathbf{z}}_{t,b}^2, \tilde{\mathbf{z}}_{t,b}^3)). \quad (3)$$

This alternating structure is repeated across all  $B$  blocks, gradually building a dense visuo-tactile representation of the joint.

### 3.2. Deformation-Aware Regularization via Virtual Force Prediction

While the predictive backbone enables joint visuo-tactile representation learning, we observe a critical modality collapse phenomenon during action training. Specifically, when the task loss can be sufficiently minimized using visual cues alone, gradients flowing through the tactile branch diminish. Consequently, the policy becomes overly reliant on vision and ignores tactile feedback, leading to unstable contact control in force-sensitive manipulation tasks [20, 33].

To counteract this issue, we introduce a deformation-aware auxiliary objective that provides direct supervision to the tactile pathway. Prior works often rely on external force-torque sensors mounted at the robot wrist or gripper to obtain ground-truth 3D force supervision [29, 48]. In contrast, we observe that vision-based tactile sensors inherently encode rich deformation patterns correlated with contact forces. By enforcing the prediction of a compact, deformation-related signal, we ensure that tactile representations remain informative without the computational overhead of reconstructing high-dimensional tactile images.

Formally, given a no-contact reference frame  $I_0$  and a current tactile frame  $I_t$ , we compute the dense optical flow  $u_t = (u_x, u_y)$ . We derive a 3D virtual force proxy  $F_t^v = [f_x, f_y, f_z]^T$  directly from this deformation field:

$$f_x = \mathbb{E}[u_x], \quad f_y = \mathbb{E}[u_y], \quad f_z = \mathbb{E}[\nabla \cdot u_t]. \quad (4)$$

Here, the spatial expectations of the flow components,  $f_x$  and  $f_y$ , encode tangential shear. Crucially,  $f_z$  approximates normal compression via flow divergence, exploiting the property that pressing a deformable elastomer against an object induces an outward expansion of the surface pattern. This signal serves as a geometrically grounded proxy rather than a calibrated physical force.

The derived virtual force  $F_t^v \in \mathbb{R}^3$  acts as an auxiliary supervision signal during action training. Instead of appending an isolated downstream prediction head, we incorporate this compact force proxy as an additional component in the joint denoising target of the conditional flow-matching objective. Specifically, the network is tasked with jointly predicting the future action and the virtual force, effectively binding the control gradients to the tactile representations. The explicit force regularization term evaluates the vector field velocity matching for the force component:

$$\mathcal{L}_{\text{force}} = \mathbb{E} \left[ \left\| v_{\theta}^f(z_t, t|c) - v^{*f} \right\|^2 \right]. \quad (5)$$

This formulation preserves deformation-sensitive information in the latent space and maintains balanced multimodal gradients throughout optimization.

### 3.3. Optimization Objective

To adapt the pretrained visual backbone for multimodal visuo–tactile modeling, we employ a two-stage training strategy. The backbone, initially pretrained exclusively on visual datasets, lacks prior exposure to the high-frequency, localized deformation patterns characteristic of tactile signals. Introducing action supervision and virtual force regularization simultaneously with modality alignment forces the network to adapt its internal representations while simultaneously optimizing a control policy.

We observe that this tight coupling induces significant distributional shifts within the backbone, degrading the quality of the tactile latents and leading to unstable convergence. To overcome this, we decouple the process: Stage I fine-tunes the backbone exclusively to model joint visuo–tactile latent dynamics, establishing a coherent multimodal world representation. Stage II then leverages this aligned representation to introduce regularized action prediction.

**Stage I: Multi-View Visuo–Tactile Latent Flow Matching.** Let  $\mathbf{z}_0$  denote the VAE-encoded latent sequence of future multi-view observations, encompassing the two camera views and the GelSight stream. We apply the flow matching formulation to model the forward dynamics of these visuo–tactile latents:

$$\mathcal{L}_{\text{stage1}} = \mathbb{E} \left[ \left\| \mathbf{v}_{\theta}(\mathbf{z}_t, t) - \mathbf{v}^* \right\|^2 \right]. \quad (6)$$

Crucially, this loss is applied exclusively to future prediction frames, while the initial conditioning frames are excluded from the optimization target. This stage adapts the pretrained backbone to capture the physical interplay between macroscopic visual dynamics and microscopic tactile deformations, ensuring a well-behaved multimodal latent space before any control signals are introduced.

**Stage II: Conditional Joint Action–State–Force Denoising.** Following the training of a robust visuo–tactile world model in Stage I, we optimize the control policy. We formulate action generation as a conditional flow-matching process. The joint denoising target is constructed by concatenating the action, virtual force, and state:

$$\mathbf{z}_0 = [\mathbf{a}; \mathbf{f}; \mathbf{s}], \quad (7)$$

where  $\mathbf{a} \in \mathbb{R}^7$  represents the 6-DoF end-effector pose and 1D gripper width,  $\mathbf{f} \in \mathbb{R}^3$  is the deformation-derived virtual force, and  $\mathbf{s} \in \mathbb{R}^{16}$  is the proprioceptive state. The network predicts the joint velocity field conditioned

on the current state token  $\mathbf{c} = [\mathbf{0}_{10}; \mathbf{s}_t]$ , where the action and force dimensions are zero-padded during conditioning. We define the flow-matching objectives for the action and state components to track the optimal denoising trajectories for their respective sub-spaces:

$$\mathcal{L}_{\text{action}} = \mathbb{E} \left[ \left\| \mathbf{v}_{\theta}^{\text{a}}(\mathbf{z}_t, t \mid \mathbf{c}) - \mathbf{v}^{*\text{a}} \right\|^2 \right], \quad (8)$$

$$\mathcal{L}_{\text{state}} = \mathbb{E} \left[ \left\| \mathbf{v}_{\theta}^{\text{s}}(\mathbf{z}_t, t \mid \mathbf{c}) - \mathbf{v}^{*\text{s}} \right\|^2 \right]. \quad (9)$$

We then integrate these with the virtual force regularization  $\mathcal{L}_{\text{force}}$  (defined previously in Eq. 5) to form the complete Stage II objective. The total loss minimizes the sum of the velocity matching errors across all three components:

$$\mathcal{L}_{\text{stage2}} = \mathcal{L}_{\text{action}} + \lambda_1 \mathcal{L}_{\text{state}} + \lambda_2 \mathcal{L}_{\text{force}}. \quad (10)$$

Because flow matching regresses a normalized velocity field ( $\epsilon - \mathbf{z}_0$ ) rather than raw data values, the target variances across the action, state, and force dimensions remain naturally scaled. This circumvents the need for the aggressive hyperparameter balancing typically required in standard MSE-based regression. Furthermore, joint state prediction introduces a vital dynamics-consistency constraint, ensuring that the model grounds its control predictions in coherent physical state transitions rather than memorizing isolated action trajectories.

## 4. Experiments

We evaluate VTAM on real-world contact-rich manipulation tasks to study the effectiveness of visuo-tactile world action modeling. Our experiments aim to answer the following key questions:

- **Q1: Effectiveness of Visuo-Tactile World Action Modeling.** Does VTAM outperform vision-only and multimodal baselines in scenarios requiring fine-grained force modulation?
- **Q2: Latent Video Fusion vs. Late-stage Injection.** Does modeling visuo-tactile dynamics within a shared video latent space offer performance advantages over late-stage tactile injection?
- **Q3: Impact of Virtual Force Regularization.** To what extent does contact-aware virtual target regularization mitigate modality collapse and stabilize multimodal training?

### 4.1. Experimental Setup

All experiments are conducted on a 6-DoF xArm6 robotic manipulator equipped with a parallel gripper (Fig. 3a). We use a GelSight Mini tactile sensor mounted on the gripper finger to capture high-resolution surface deformation. Visual observations are obtained from two Intel RealSense D455 RGB-D cameras mounted in a dual-head configuration. Both data collection and action execution run at 30 Hz. We compare VTAM against several strong baselines to evaluate the effectiveness of visuo-tactile world action modeling.

- **Video-Action Model (Genie Envisioner) [19].** A state-of-the-art video foundation model that integrates an instruction-conditioned video diffusion backbone with a flow-matching action decoder.
- $\pi_{0.5}$  (**Vision-Only**) [24]. The official implementation of the  $\pi_{0.5}$  generalist Vision-Language-Action (VLA) policy, which scales the  $\pi_0$  architecture [3] for open-world generalization. This baseline isolates the performance limits of semantic-heavy, vision-only representations in force-sensitive scenarios where critical contact states are visually occluded.
- $\pi_{0.5}$  + **Naïve Tactile Injection** [24]. A multimodal extension of the  $\pi_{0.5}$  architecture where the high-dimensional GelSight tactile stream is injected simply as an additional visual view. This setup is specifically



(a) Robot experiment setup.

(b) Manual data collection.

**Figure 3: Experiment setup and data acquisition.** We collect demonstrations through manual teleoperation using a visuo-tactile sensing setup for contact-rich manipulation tasks such as chip pick-and-place.

included to demonstrate the modality collapse phenomenon, where dominant visual gradients suppress localized tactile signals during unregularized joint training.

#### 4.2. Real-World Tasks and Data Collection

We evaluate VTAM on three contact-rich manipulation tasks:

- **Potato Chip Pick-and-Place:** Grasping and transporting fragile potato chips without breakage, requiring fine-grained force modulation. Success depends on precisely regulating grasp force and detecting contact onset under severe hand-induced occlusion. The policy must avoid both under-grasping (slip/drop) and over-grasping (chip fracture) while lifting and placing.
- **Cucumber Peeling:** Maintaining stable contact while peeling a deformable vegetable, demanding continuous shear-force control. This task requires sensitivity to small changes in friction and deformation as the tool slides.
- **Whiteboard Wiping:** Using a rigid whiteboard eraser to wipe a flat or inclined surface, requiring sustained contact and precise normal force regulation to prevent chatter and lift-off.

For evaluation, we collect a real-world visuo-tactile dataset for these tasks using a dual-camera setup and a GelSight sensor (Fig. 3b). The dataset consists of 100 chip pick-and-place, 105 whiteboard wiping, and 61 peeling trajectories. All demonstrations are collected through manual teleoperation and include synchronized multi-view RGB streams, tactile deformation images, and robot state information.

#### 4.3. Quantitative Results (Q1)

For evaluation, we conduct 20 trials per task. The tasks include chip pick-and-place, flat whiteboard wiping with a rigid eraser, tilted whiteboard wiping, and cucumber peeling. In total, each model is evaluated on 80 real-world trials, with inference performed at 1 Hz. Table 1 reports the performance comparison across contact-rich manipulation tasks. Overall, VTAM significantly outperforms baselines, achieving success rates of **90%**, **85%**, and **95%** on chip pick-and-place, cucumber peeling, and whiteboard wiping, respectively.

**Table 1: Overall performance comparison.**

Model	Chip	Peel	Wipe
Genie Envisioner	0%	0%	2.5%
$\pi_{0.5}$ (Vision)	10%	0%	0%
$\pi_{0.5}$ + Tactile	5%	0%	0%
<b>VTAM (Ours)</b>	<b>90%</b>	<b>85%</b>	<b>95%</b>

On the chip pick-and-place task, VTAM achieves a success rate of 90%, demonstrating strong robustness in brittle-object manipulation where accurate grasp verification and force control are required. In contrast, baselines frequently fail to detect unsuccessful grasps and proceed directly to the placement stage.

For cucumber peeling, VTAM reaches 85% success while all baselines fail to complete the task, confirming tactile feedback is essential for maintaining stable contact and regulating shear forces when interacting with deformable objects.

On the whiteboard wiping task, VTAM achieves 95% success across both flat and tilted surfaces, whereas baseline methods either apply unstable contact forces or fail to maintain consistent surface following. These results highlight the importance of visuo-tactile world action modeling for robust force regulation in contact-rich manipulation.

#### 4.4. Qualitative Examples and Failure Mode Analysis

Figure 4 shows qualitative comparisons across the three tasks. We analyze the behaviors of different methods to understand how VTAM addresses the challenges in contact-rich tasks. Additional examples can be found in the Appendix.

**Chip Pick-and-Place.** For the GE vision-only baseline, the main failure arises from the inability to verify successful grasps. The robot often closes the gripper above the chip and proceeds to the plate even when the grasp fails. The Pi variants with and without tactile input exhibit similar behaviors, indicating that methods without effective tactile signal integration cannot perform correct force-aware grasping. In contrast, VTAM exhibits tactile-aware behaviors. The robot lifts the chip only when tactile deformation confirms successful contact and maintains a stable gripper width to prevent dropping during lifting. In case the grasp fails, the policy can also detect the absence of tactile signals during lifting and immediately return to the chip to reattempt the grasp, rather than continuing to the plate and releasing the gripper.

**Cucumber Peeling.** The GE baseline and both Pi variants exhibit similar motion patterns. Starting from the left side of the cucumber, the tool first moves toward the centerline and then moves away from it while sliding along the surface. This trajectory resembles a vision-driven strategy that attempts to follow the object curvature rather than regulating contact force. As a result, the tool frequently loses contact with the cucumber surface. In contrast, our VTAM policy establishes stable contact and maintains proper force while moving along the surface. The robot can perform repeated peeling motions at the same location, demonstrating accurate perception of contact states even when the cucumber thickness varies.

**Whiteboard Wiping.** On both flat and tilted whiteboards, the two Pi variants apply excessively large contact forces, sometimes even pushing the books used to support the tilted board out of place. This behavior likely arises because the training data contains both flat and tilted surfaces, making it difficult for the model to infer the correct end-effector height from visual observations alone. As a result, the policy cannot reliably determine when the gripper should move downward to follow a lower surface or remain higher to accommodate a tilted plane, and instead compensates by applying excessive force to maintain contact.

In terms of the GE baseline, although it occasionally performs light wiping motions on flat surfaces, the contact becomes unstable and the end-effector motion turns irregular on tilted boards. The policy tends to follow a trajectory suitable for flat surfaces, causing the end-effector to press excessively against higher regions of the tilted board while failing to maintain stable contact when the surface height changes. In contrast, VTAM maintains moderate and stable contact forces on both flat and tilted surfaces, enabling consistent wiping and effective stain removal. This reflects that VTAM can effectively leverage tactile information to handle visually ambiguous contact-rich tasks.

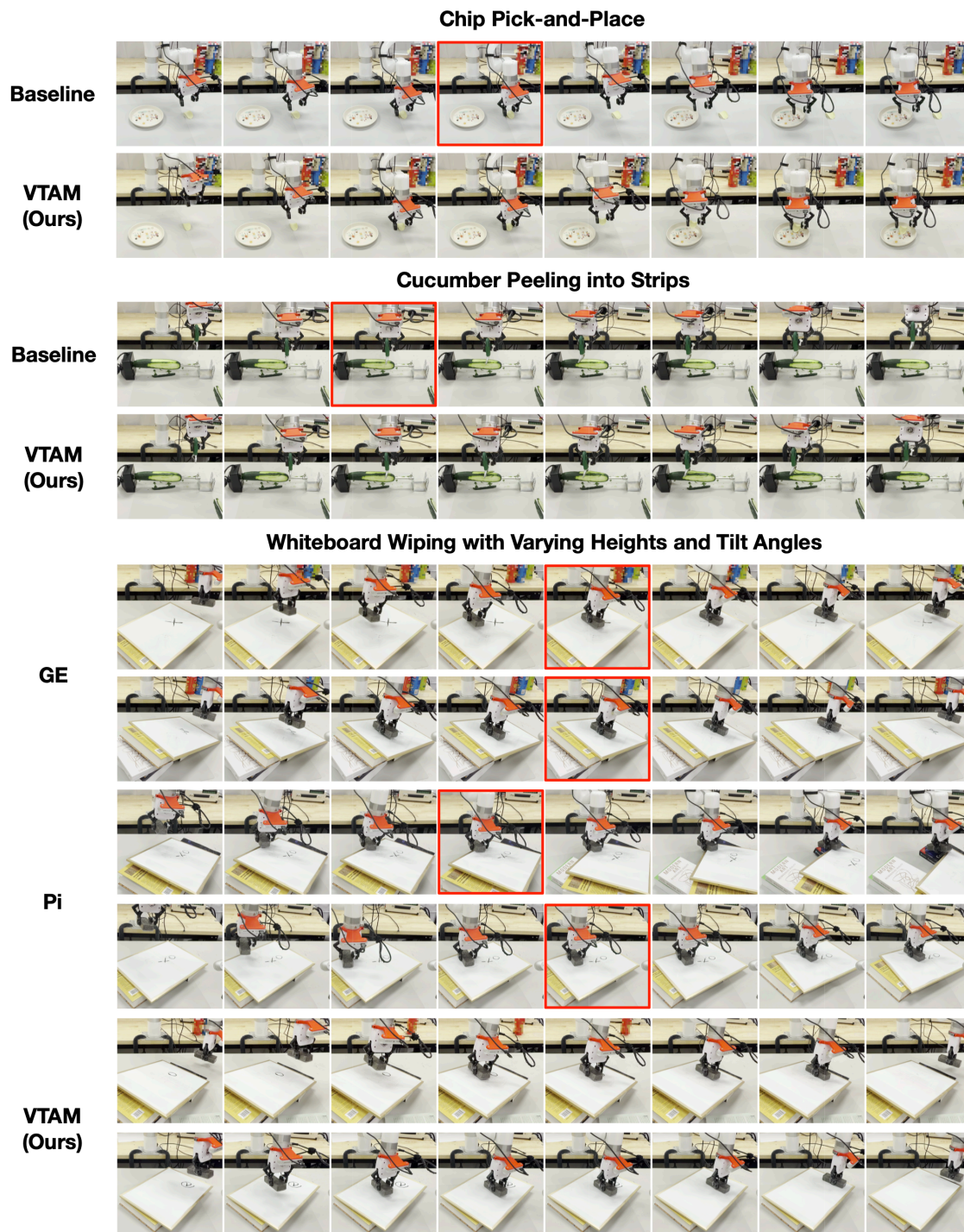


**Figure 4: Qualitative comparison between VTAM and baseline methods on real-world manipulation tasks.** Top: *Chip pick-and-place*. Vision-only baselines fail to determine whether the chip has been successfully grasped and proceed to the placement stage even when the grasp fails. Middle: *Cucumber peeling into strips*. Baselines tend to follow a vision-driven trajectory that approaches the center of the cucumber but fail to maintain consistent contact with the surface, indicating poor force regulation and lack of contact awareness. Bottom: *Whiteboard wiping under varying heights and tilt angles*. Baselines exhibit unstable wiping behaviors, often applying either insufficient or excessively large forces, particularly on tilted surfaces. In contrast, VTAM maintains stable contact and appropriate force regulation across all tasks, enabling robust manipulation behaviors. Red boxes highlight representative failure cases of baselines.

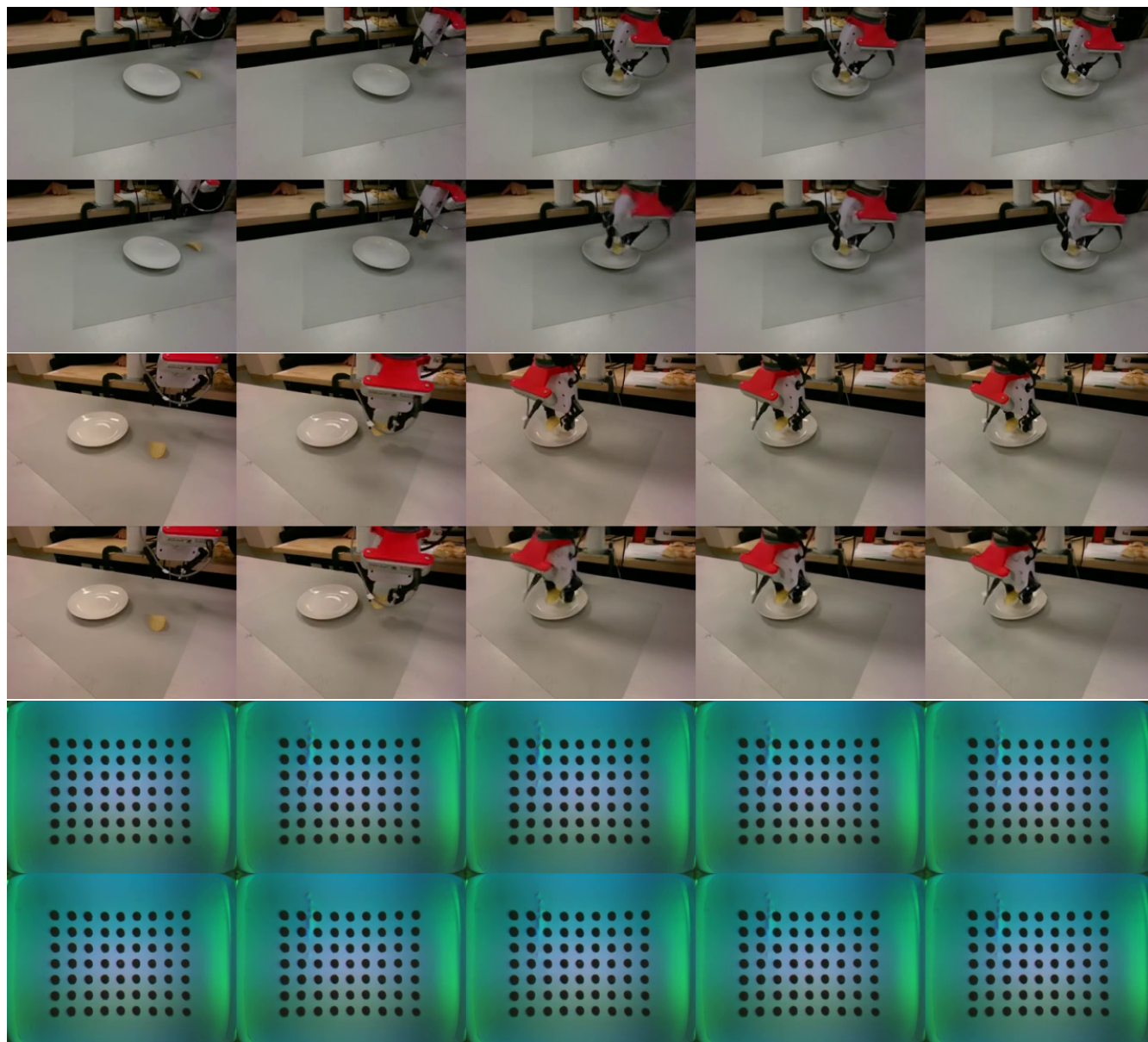


**Figure 5: Prediction visualization of the backbone video model.** From top to bottom: Camera-1 view, Camera-2 view, Tactile stream prediction. Ground-truth (top rows) and VTAM predictions (bottom rows).

#### 4.5. Prediction Visualization

We visualize the predictions of the backbone video model in Fig. 5. For each view and tactile prediction, the top row shows ground-truth frames while the bottom row shows model predictions. The model preserves cross-view temporal consistency and in-view dynamics, with only minor blurring in details irrelevant to manipulation, indicating reliable visuo-tactile world modeling for action generation.

**Table 2:** Ablation study on the Chip Pick-and-Place task (10 trials per variant).

Model Variant	Tactile Integration	Success Rate
Vision-only (No Tactile)	None	0%
Late-Fusion Tactile	Downstream Only	0%
No Virtual-Force Reg.	Joint Latent	10%
<b>VTAM (Ours)</b>	<b>Hierarchical World Model</b>	<b>90%</b>

#### 4.6. Ablation Study on Chip Pick-and-Place Task (Q2 & Q3)

To evaluate VTAM’s architectural components, we conduct ablations on the contact-sensitive Chip Pick-and-Place task at a constrained 1 Hz inference frequency (Table 2). The full VTAM model achieves 90% success rate, utilizing predictive world modeling to anticipate interaction states between low-frequency sensory updates. In contrast, all ablations fail to reliably secure the fragile chip. The *Vision-only* baseline yields a 0% success rate, as visual depth estimation suffers from severe occlusion during the final approach and cannot perceive subtle contact transitions. Introducing tactile signals only at the action head (*Late-Fusion*) also results in 0% success (Q2), demonstrating that raw force injection is insufficient without our hierarchical visuo–tactile world modeling. Finally, removing the virtual-force regularization (*No Reg.*) drops performance to 10% due to “vision modality dominance” (Q3), confirming that this auxiliary loss is critical for preventing representation collapse and ensuring tactile signals influence the entire denoising process.

## 5. Conclusion

We introduce VTAM, a visuo–tactile world action model for contact-rich manipulation. VTAM trains a predictive backbone to model the joint evolution of multi-view video and high-resolution tactile signals, so the policy can use contact dynamics that are weakly observable or occluded in vision. This predictive formulation learns temporally consistent contact features without requiring explicit labels for contact events and avoids relying on purely downstream, reactive tactile fusion. To prevent the common failure mode where action training defaults to visual cues and suppresses tactile information, we add a deformation-derived virtual-force prediction objective that maintains tactile supervision through the control pathway. On real robot tasks that demand precise force regulation, including chip pick-and-place and cucumber peeling, VTAM substantially improves success rate and interaction stability over vision-only and naive tactile baselines, highlighting the importance of modeling contact dynamics directly for reliable physical interaction. Ultimately, our framework provides a scalable, physically grounded approach to embodied intelligence, proving that predictive joint modeling is essential for reliable execution in complex physical interactions.

---

## References

- [1] Suneel Belkhale, Tianli Ding, Ted Xiao, Pierre Sermanet, Quon Vuong, Jonathan Tompson, Yevgen Chebotar, Debidatta Dwibedi, and Dorsa Sadigh. Rt-h: Action hierarchies using language. *arXiv preprint arXiv:2403.01823*, 2024.
- [2] Jianxin Bi, Kevin Yuchen Ma, Ce Hao, Mike Zheng Shou, and Harold Soh. VLA-Touch: Enhancing vision-language-action models with dual-level tactile feedback. *arXiv preprint arXiv:2507.17294*, 2025.
- [3] Kevin Black, Noah Brown, Danny Driess, Adnan Esmail, Michael Equi, Chelsea Finn, Niccolo Fusai, Lachy Groom, Karol Hausman, Brian Ichter, et al.  $\pi_0$ : A vision-language-action flow model for general robot control. *arXiv preprint arXiv:2410.24164*, 2024.
- [4] Anthony Brohan, Noah Brown, Justice Carbajal, Yevgen Chebotar, Joseph Dabis, Chelsea Finn, Keerthana Gopalakrishnan, Karol Hausman, Alex Herzog, Jasmine Hsu, et al. Rt-1: Robotics transformer for real-world control at scale. *arXiv preprint arXiv:2212.06817*, 2022.
- [5] Jake Bruce et al. Genie: Generative interactive environments. *arXiv preprint arXiv:2402.15391*, 2024.
- [6] Wendi Chen, Han Xue, Yi Wang, Fangyuan Zhou, Jun Lv, Yang Jin, Shirun Tang, Chuan Wen, and Cewu Lu. Implicitrdp: An end-to-end visual-force diffusion policy with structural slow-fast learning. *arXiv preprint arXiv:2512.10946*, 2025.
- [7] Vedant Dave, Fotios Lygerakis, and Elmar Rueckert. Multimodal visual-tactile representation learning through self-supervised contrastive pre-training. In *International Conference on Robotics and Automation (ICRA)*, pages 8013–8020, 2024.
- [8] Siyuan Dong, Wenzhen Yuan, and Edward H Adelson. Improved gelsight tactile sensor for measuring geometry and slip. In *International Conference on Intelligent Robots and Systems (IROS)*, pages 137–144, 2017.
- [9] Danny Driess, Fei Xia, Mehdi SM Sajjadi, Corey Lynch, Aakanksha Chowdhery, Brian Ichter, Ayzaan Wahid, Jonathan Tompson, Quan Vuong, Tianhe Yu, et al. Palm-e: An embodied multimodal language model. *arXiv preprint arXiv:2303.03378*, 2023.
- [10] Yoav HaCohen et al. Ltx-video: Realtime video latent diffusion. *arXiv preprint arXiv:2501.00103*, 2024.
- [11] Peng Hao, Chaofan Zhang, Dingzhe Li, Xiaoge Cao, Xiaoshuai Hao, Shaowei Cui, and Shuo Wang. Tla: Tactile-language-action model for contact-rich manipulation. *arXiv preprint arXiv:2503.08548*, 2025.
- [12] Kaiming He, Xiangyu Zhang, Shaoqing Ren, and Jian Sun. Deep residual learning for image recognition. In *IEEE Conference on Computer Vision and Pattern Recognition (CVPR)*, pages 770–778, 2016.
- [13] Carolina Higuera, Akash Sharma, Chaithanya Krishna Bodduluri, Taosha Fan, Patrick Lancaster, Mrinal Kalakrishnan, Michael Kaess, Byron Boots, Mike Lambeta, Tingfan Wu, et al. Sparsh: Self-supervised touch representations for vision-based tactile sensing. *arXiv preprint arXiv:2410.24090*, 2024.
- [14] Binghao Huang, Yixuan Wang, Xinyi Yang, Yiyue Luo, and Yunzhu Li. 3d-vitac: Learning fine-grained manipulation with visuo-tactile sensing. *arXiv preprint arXiv:2410.24091*, 2024.
- [15] Binghao Huang, Jie Xu, Iretiayo Akinola, Wei Yang, Balakumar Sundaralingam, Rowland O’Flaherty, Dieter Fox, Xiaolong Wang, Arsalan Mousavian, Yu-Wei Chao, et al. Vt-refine: Learning bimanual assembly with visuo-tactile feedback via simulation fine-tuning. *arXiv preprint arXiv:2510.14930*, 2025.

- 
- [16] Jialei Huang, Shuo Wang, Fanqi Lin, Yihang Hu, Chuan Wen, and Yang Gao. Tactile-VLA: Unlocking vision-language-action model’s physical knowledge for tactile generalization. *arXiv preprint arXiv:2507.09160*, 2025.
- [17] Moo Jin Kim, Karl Pertsch, Siddharth Karamcheti, Ted Xiao, Ashwin Balakrishna, Suraj Nair, Rafael Rafailov, Ethan Foster, Grace Lam, Pannag Sanketi, et al. OpenVLA: An open-source vision-language-action model. *arXiv preprint arXiv:2406.09246*, 2024.
- [18] Diederik P Kingma and Max Welling. Auto-encoding variational bayes. *arXiv preprint arXiv:1312.6114*, 2013.
- [19] Yue Liao, Pengfei Zhou, Siyuan Huang, Donglin Yang, Shengcong Chen, Yuxin Jiang, Yue Hu, Jingbin Cai, Si Liu, Jianlan Luo, et al. Genie envisioner: A unified world foundation platform for robotic manipulation. *arXiv preprint arXiv:2508.05635*, 2025.
- [20] Jason Jingzhou Liu, Yulong Li, Kenneth Shaw, Tony Tao, Ruslan Salakhutdinov, and Deepak Pathak. Factr: Force-attending curriculum training for contact-rich policy learning. *arXiv preprint arXiv:2502.17432*, 2025.
- [21] Ilya Loshchilov and Frank Hutter. Decoupled weight decay regularization. *arXiv preprint arXiv:1711.05101*, 2017.
- [22] Amit Parag, Edward H Adelson, and Ekrem Misimi. Learning incipient slip with gelsight sensors: Attention classification with video vision transformers. In *International Conference on Intelligent Robots and Systems (IROS)*, pages 13960–13966, 2024.
- [23] Jeongeun Park, Jihwan Yoon, Byungwoo Jeon, Juhan Park, Jinwoo Shin, Namhoon Cho, Kyungjae Lee, Sangdoon Yun, and Sungjoon Choi. Hierarchical vision language action model using success and failure demonstrations. *arXiv preprint arXiv:2512.03913*, 2025.
- [24] Physical Intelligence, Kevin Black, Noah Brown, James Darpinian, Karan Dhabalia, Danny Driess, Adnan Esmail, Michael Equi, Chelsea Finn, Niccolo Fusai, et al.  $pi_{0.5}$ : a vision-language-action model with open-world generalization. *arXiv preprint arXiv:2504.16054*, 2025.
- [25] Samyam Rajbhandari, Jeff Rasley, Olatunji Ruwase, and Yuxiong He. Zero: Memory optimizations toward training trillion parameter models. In *SC20: International Conference for High Performance Computing, Networking, Storage and Analysis*, pages 1–16. IEEE, 2020.
- [26] Younggyo Seo, Danijar Hafner, Hao Liu, Fangchen Liu, Stephen James, Kimin Lee, and Pieter Abbeel. Masked world models for visual control. In *Conference on Robot Learning (CoRL)*, pages 1332–1344, 2023.
- [27] Zilin Si, Gu Zhang, Qingwei Ben, Branden Romero, Zhou Xian, Chao Liu, and Chuang Gan. Diff tactile: A physics-based differentiable tactile simulator for contact-rich robotic manipulation. *arXiv preprint arXiv:2403.08716*, 2024.
- [28] Lin Sun, Bin Xie, Yingfei Liu, Hao Shi, Tiancai Wang, and Jiale Cao. Geovla: Empowering 3d representations in vision-language-action models. *arXiv preprint arXiv:2508.09071*, 2025.
- [29] Balakumar Sundaralingam, Alexander Sasha Lambert, Ankur Handa, Byron Boots, Tucker Hermans, Stan Birchfield, Nathan Ratliff, and Dieter Fox. Robust learning of tactile force estimation through robot interaction. In *International Conference on Robotics and Automation (ICRA)*, pages 9035–9042, 2019.
-

- 
- [30] Octo Model Team, Dibya Ghosh, Homer Walke, Karl Pertsch, Kevin Black, Oier Mees, Sudeep Dasari, Joey Hejna, Tobias Kreiman, Charles Xu, et al. Octo: An open-source generalist robot policy. *arXiv preprint arXiv:2405.12213*, 2024.
- [31] Pascal Vincent, Hugo Larochelle, Yoshua Bengio, and Pierre-Antoine Manzagol. Extracting and composing robust features with denoising autoencoders. In *International Conference on Machine Learning (ICML)*, pages 1096–1103, 2008.
- [32] Qiang Wang, Pablo Martinez Ulloa, Robert Burke, David Cordova Bulens, and Stephen J Redmond. Robust learning-based incipient slip detection using the papillarray optical tactile sensor for improved robotic gripping. *IEEE Robotics and Automation Letters*, 9(2):1827–1834, 2023.
- [33] Weiyao Wang, Du Tran, and Matt Feiszli. What makes training multi-modal classification networks hard? In *IEEE Conference on Computer Vision and Pattern Recognition (CVPR)*, pages 12695–12705, 2020.
- [34] Nan Wu, Stanislaw Jastrzebski, Kyunghyun Cho, and Krzysztof J Geras. Characterizing and overcoming the greedy nature of learning in multi-modal deep neural networks. In *International Conference on Machine Learning (ICML)*, pages 24043–24055, 2022.
- [35] Zhengtong Xu, Raghava Uppuluri, Xinwei Zhang, Cael Fitch, Philip Glen Crandall, Wan Shou, Dongyi Wang, and Yu She. Unit: Data efficient tactile representation with generalization to unseen objects. *IEEE Robotics and Automation Letters*, 2025.
- [36] Han Xue, Jieji Ren, Wendi Chen, Gu Zhang, Yuan Fang, Guoying Gu, Huazhe Xu, and Cewu Lu. Reactive diffusion policy: Slow-fast visual-tactile policy learning for contact-rich manipulation. *arXiv preprint arXiv:2503.02881*, 2025.
- [37] Fengyu Yang, Chao Feng, Ziyang Chen, Hyungseob Park, Daniel Wang, Yiming Dou, Ziyao Zeng, Xien Chen, Rit Gangopadhyay, Andrew Owens, et al. Binding touch to everything: Learning unified multimodal tactile representations. In *IEEE Conference on Computer Vision and Pattern Recognition (CVPR)*, pages 26340–26353, 2024.
- [38] Ze Yang, Yun Chen, Jingkan Wang, Sivabalan Manivasagam, Wei-Chiu Ma, Anqi Joyce Yang, and Raquel Urtasun. Unisim: A neural closed-loop sensor simulator. In *IEEE Conference on Computer Vision and Pattern Recognition (CVPR)*, pages 1389–1399, 2023.
- [39] Seonghyeon Ye, Yunhao Ge, Kaiyuan Zheng, Shenyuan Gao, Sihyun Yu, George Kurian, Suneel Indupuru, You Liang Tan, Chuning Zhu, Jiannan Xiang, et al. World action models are zero-shot policies. *arXiv preprint arXiv:2602.15922*, 2026.
- [40] Jiawen Yu, Hairuo Liu, Qiaojun Yu, Jieji Ren, Ce Hao, Haitong Ding, Guangyu Huang, Guofan Huang, Yan Song, Panpan Cai, et al. Forcevla: Enhancing vla models with a force-aware moe for contact-rich manipulation. *arXiv preprint arXiv:2505.22159*, 2025.
- [41] Wenzhen Yuan, Siyuan Dong, and Edward H Adelson. Gelsight: High-resolution tactile sensors for perceiving physical properties. *IEEE Robotics & Automation Magazine*, 24(3):66–77, 2017.
- [42] Brayan S Zapata-Impata, Pablo Gil, and Fernando Torres. Learning spatio temporal tactile features with a convlstm for the direction of slip detection. *Sensors*, 19(3):523, 2019.
-

- [43] Chaofan Zhang, Peng Hao, Xiaoge Cao, Xiaoshuai Hao, Shaowei Cui, and Shuo Wang. VTLA: Vision-tactile-language-action model with preference learning for insertion manipulation. *arXiv preprint arXiv:2505.09577*, 2025.
- [44] Wenyao Zhang, Hongsi Liu, Zekun Qi, Yunnan Wang, Xinqiang Yu, Jiazhao Zhang, Runpei Dong, Jiawei He, Fan Lu, He Wang, et al. DreamVLA: a vision-language-action model dreamed with comprehensive world knowledge. *arXiv preprint arXiv:2507.04447*, 2025.
- [45] Zongzheng Zhang, Haobo Xu, Zhuo Yang, Chenghao Yue, Zehao Lin, Huan-ang Gao, Ziwei Wang, and Hao Zhao. Ta-vla: Elucidating the design space of torque-aware vision-language-action models. *arXiv preprint arXiv:2509.07962*, 2025.
- [46] Haoyu Zhen, Xiaowen Qiu, Peihao Chen, Jincheng Yang, Xin Yan, Yilun Du, Yining Hong, and Chuang Gan. 3d-vla: A 3d vision-language-action generative world model. *arXiv preprint arXiv:2403.09631*, 2024.
- [47] Chuning Zhu, Raymond Yu, Siyuan Feng, Benjamin Burchfiel, Paarth Shah, and Abhishek Gupta. Unified world models: Coupling video and action diffusion for pretraining on large robotic datasets. *arXiv preprint arXiv:2504.02792*, 2025.
- [48] Yifan Zhu, Mei Hao, Xupeng Zhu, Quentin Bateux, Alex Wong, and Aaron M Dollar. Forces for free: Vision-based contact force estimation with a compliant hand. *Science Robotics*, 10(103):eadq5046, 2025.
- [49] Brianna Zitkovich, Tianhe Yu, Sichun Xu, Peng Xu, Ted Xiao, Fei Xia, Jialin Wu, Paul Wohlhart, Stefan Welker, Ayzaan Wahid, et al. RT-2: Vision-language-action models transfer web knowledge to robotic control. In *Conference on Robot Learning (CoRL)*, pages 2165–2183, 2023.

## A. Training Details

**VTAM World Model.** The VTAM model is trained in two stages on  $4\times$  NVIDIA A100 GPUs (40 GB VRAM each) using DeepSpeed ZeRO Stage 2 [25] with bf16 mixed precision. In *Stage 1: Video-only pre-training*, the video prediction backbone is initialized from a pre-trained Genie Envisioner (GE-base) checkpoint [19], an LTX-Video transformer [10] with 28 layers, 32 attention heads, and hidden dimension 2048, and fine-tuned for 50,000 steps using the video-only objective (`train_mode=video_only`). We set  $B = 28$  following the default configuration of the pretrained LTX-Video backbone. This choice ensures compatibility with the pretrained architecture and maintains stable training behavior. We employ AdamW [21] ( $\beta_1 = 0.9$ ,  $\beta_2 = 0.95$ , weight decay  $10^{-5}$ ) with a constant learning rate of  $3 \times 10^{-4}$  after 1,000 warmup steps, gradient clipping ( $\|\nabla\| = 1.0$ ), and a per-GPU batch size of 16. In *Stage 2: Action head training*, an action expert head is appended to the frozen video backbone. The action expert is implemented as a parallel Transformer branch consisting of 28 layers, mirroring the depth of the video backbone. Each layer contains (i) a self-attention module over action-state tokens, (ii) a cross-attention module attending to the corresponding layer’s video hidden states, and (iii) a feed-forward network. All modules are modulated using adaptive layer normalization (AdaLN) conditioned on the diffusion timestep. This stage is trained for 20,000 steps using the action-full objective with a lower learning rate of  $5 \times 10^{-5}$  (constant with 1,000 warmup steps), while keeping all other hyperparameters identical to Stage 1. Training is performed using Flow Matching with the Euler Discrete Scheduler, achieving approximately 3.4 s per optimization step. For the chip pick-and-place, cucumber peeling, and whiteboard wiping tasks, video inputs are resized to  $192 \times 256$  with a temporal chunk size of 9 frames and an action chunk size of 54. Actions are represented in absolute joint space (*i.e.*, target joint positions rather than deltas) and normalized using pre-computed per-dimension statistics. We apply caption dropout ( $p = 0.06$ ) and first-frame noise injection (scale 0.1) for regularization.

**Optimization Details.** We set the total loss coefficients to  $\lambda_1 = \lambda_2 = 1$  for all experiments. Since all three objectives share the same flow-matching formulation, implemented as mean squared error on predicted velocity fields in normalized latent space, their magnitudes remain on comparable scales. Therefore, equal weighting provides a stable and straightforward choice without introducing additional hyperparameters.

**GE-Act Baseline.** The Vision-only GE-Act baseline [19] follows the same two-stage training protocol as VTAM. In Stage 1, the LTX-Video transformer backbone is initialized from the GE-base checkpoint and fine-tuned for 50,000 steps using the video-only objective. We employ AdamW ( $\beta_1 = 0.9$ ,  $\beta_2 = 0.95$ , weight decay  $10^{-5}$ ) with a constant learning rate of  $3 \times 10^{-4}$  after 1,000 warmup steps, gradient clipping ( $\|\nabla\| = 1.0$ ), and a per-GPU batch size of 16. In Stage 2, a randomly initialized action expert head is appended and trained for 20,000 steps using the action-full objective with a lower learning rate of  $5 \times 10^{-5}$  (constant with 1,000 warmup steps). All remaining settings, including video resolution ( $192 \times 256$ ), temporal chunk size (9 frames), action chunk size (54), bf16 precision, DeepSpeed ZeRO Stage 2, and Flow Matching with the Euler Discrete Scheduler, are identical to those used in VTAM training.

**$\pi_{0.5}$  Policy.** The  $\pi_{0.5}$  policies [24] are fine-tuned from a pre-trained  $\pi_{0.5}$  base checkpoint on  $4\times$  NVIDIA A100 GPUs (40 GB VRAM each) using Fully Sharded Data Parallel (FSDP) with bfloat16 mixed precision. We optimize the models using AdamW ( $\beta_1 = 0.9$ ,  $\beta_2 = 0.95$ ) with a peak learning rate of  $2.5 \times 10^{-5}$  following a cosine decay schedule with 1,000 warmup steps, decaying to  $2.5 \times 10^{-6}$  over 30,000 steps. Gradient clipping is applied with  $\|\nabla\| = 1.0$ . The global batch size is set to 64, and we use an exponential moving average (EMA) with decay 0.999. The action dimension is 32 with an action horizon of 50. Input images are resized to  $224 \times 224$ . States and actions are normalized using quantile normalization with pre-computed dataset statistics. All task-specific models are trained for 10,000 optimization steps.

## B. Experimental Details

**Evaluation Protocol.** We evaluate each policy using real-world success rate over multiple independent trials. For all tasks, the robot executes the policy under randomized initial conditions, and success is determined according to task-specific criteria.

**Chip Pick-and-Place.** The policy is evaluated over 20 consecutive trials. In each trial, the potato chip is placed at a random initial position. The robot must move above the potato chip, grasp it without damage, and place it into the target plate. A trial is counted as a failure if the robot fails to grasp, breaks the chip, or drops it during transport.

**Whiteboard Wiping.** We evaluate the wiping task under two board inclination settings:  $0^\circ$  (flat) and  $45^\circ$  (inclined). A random black stain is drawn at the start of each trial. The robot is allowed at most five wiping motions. Success is defined as the complete removal of the stain without disturbing the board or its supports. Each setting is evaluated over 20 trials.

**Cucumber Peeling.** For the peeling task, the robot performs 20 consecutive motions at a fixed cutting position. As the cucumber is peeled, its height decreases, requiring the robot to dynamically adjust contact force. As shown in Fig. 6, 17 out of 20 trials (85% success rate) produced peel strips longer than 10cm, demonstrating the VTAM’s ability to maintain stable contact despite changing geometry.

## C. Video Prediction Examples

We visualize qualitative video prediction results for two contact-rich manipulation tasks: cucumber peeling and whiteboard wiping. To evaluate visual fidelity, we compare predicted frames against ground truth for the rear camera (Fig. 7 and Fig. 10) and front camera (Fig. 8 and Fig. 11). Furthermore, we assess the model’s ability to anticipate contact dynamics by predicting tactile streams (Fig. 9 and Fig. 12). Yellow arrows in the tactile plots visualize estimated contact force magnitude and direction. Note that these are for visualization purposes only; the model processes raw tactile tokens without explicit force inputs. Results demonstrate that VTAM effectively captures both visual motion and fine-grained contact dynamics across modalities.



**Figure 6: Qualitative peeling results.** VTAM achieves an 85% success rate (17/20 trials), producing peel strips longer than 10 cm in successful runs.



**Figure 7: Cucumber peeling video prediction (rear camera view).** Top row: ground-truth; Bottom row: model predictions. The predicted frames closely match the ground-truth observations.

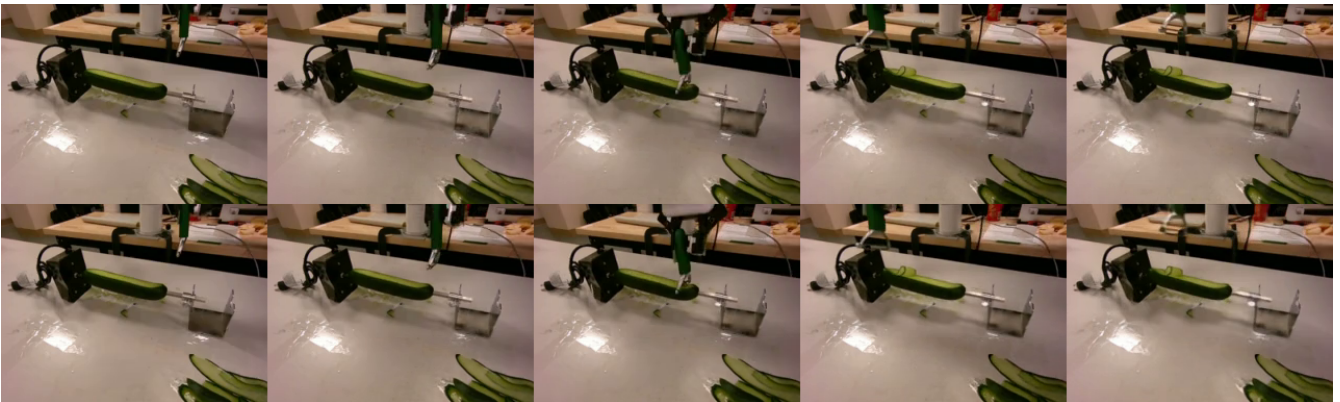


**Figure 8: Cucumber peeling video prediction (front camera view).** The model maintains consistency with the ground truth across the manipulation sequence.

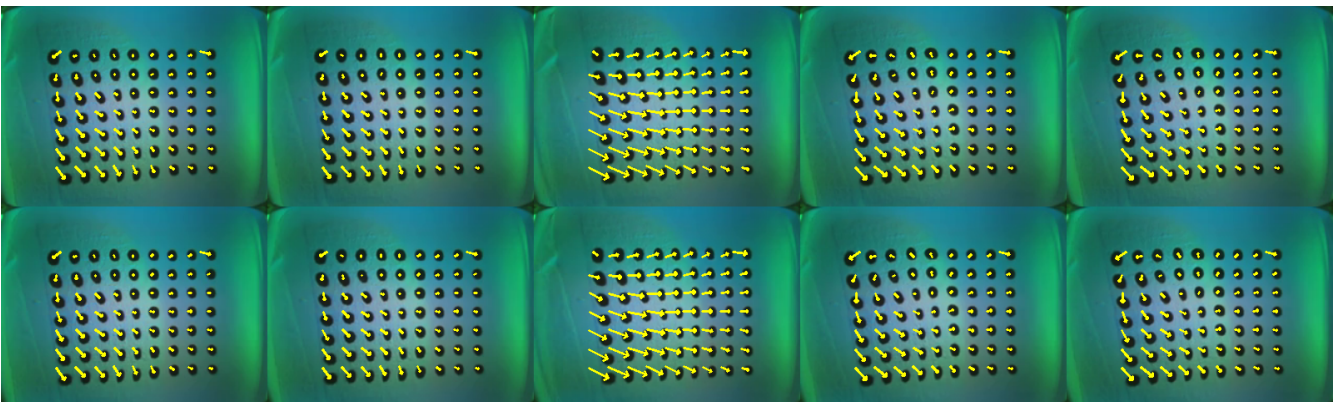


**Figure 9: Cucumber peeling tactile prediction.** Tactile frames are predicted accurately. Yellow arrows visualize estimated forces for interpretation only.



Figure 10: Whiteboard wiping video prediction (rear camera view). Top row: ground-truth; Bottom row: model predictions. Predictions match the ground truth across the wiping motion.

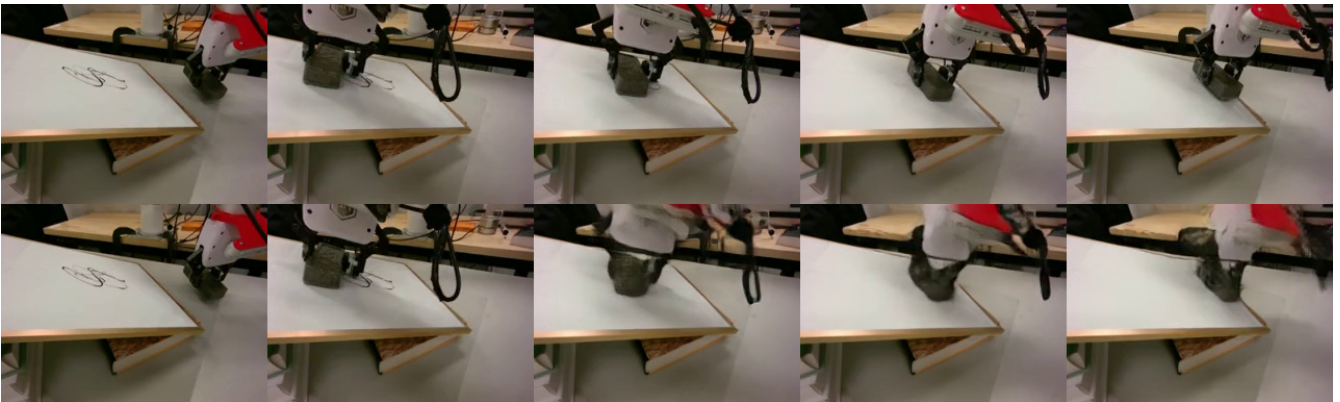


Figure 11: Whiteboard wiping video prediction (front camera view). The model successfully reproduces the visual dynamics of the wiping interaction.

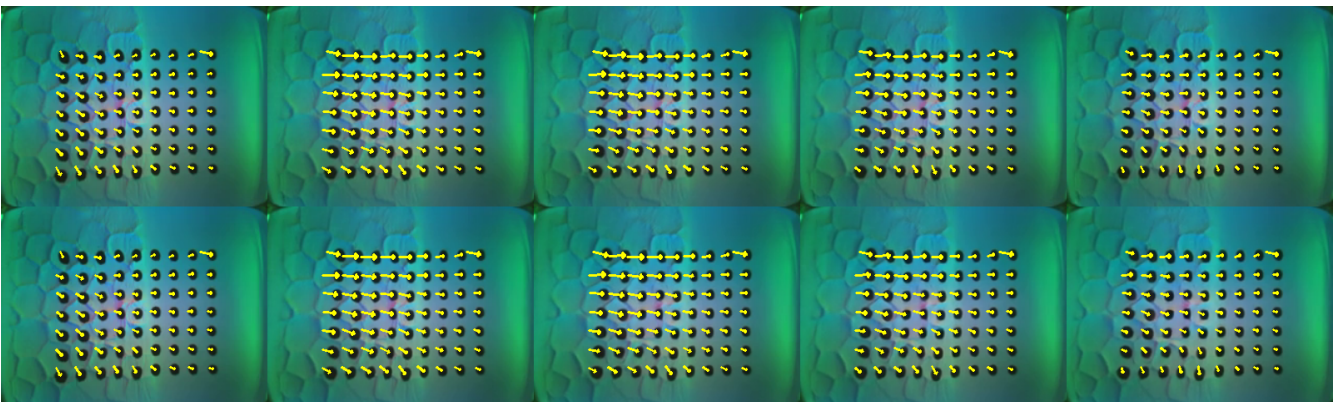


Figure 12: Whiteboard wiping tactile prediction. The predicted tactile frames capture the interaction between the wiper and the board surface.